# Distributed modal birefringence measurement in a few-mode fiber based on stimulated Brillouin scattering

E. Catalano, R. Vallifuoco, L. Zeni, M. Cappelletti, A. Galtarossa, L. Palmieri, A. Minardo

***Abstract*—We present a novel method to characterize the modal birefringence in a few-mode fiber (FMF), based on stimulated Brillouin scattering. The method exploits two phenomena which can be observed in distributed Brillouin measurements: the dependence of the Brillouin frequency shift (BFS) on the effective refractive index (ERI) of the interacting optical beams, and the spatial oscillations of the Brillouin gain along the FMF deriving from multimodal interference. Using both phenomena, a wide range of ERI separations can be measured, from ≈ $10^{-7}$ to $10^{-2}$ or more. The method has been demonstrated over a two-mode graded-index FMF, using two photonic lanterns to selectively excite the desired spatial modes. The birefringence values obtained using the proposed method have been validated using a different distributed technique, based on the analysis of the fiber's Rayleigh-backscattered trace acquired in the frequency domain.**

***Index Terms*—Stimulated Brillouin scattering, modal birefringence, few-mode fibers.**

## I. Introduction

THE characterization of the distributed modal birefringence in few-mode fibers (FMF) is of great interest in both space-division-multiplexing (SDM) [1] and fiber sensing [2]. Different techniques have been demonstrated to characterize these fibers, based on either Rayleigh [3-4] or Brillouin scattering [5-6]. Rayleigh-based configurations for FMF characterization include phase-sensitive time-domain [3], and frequency-domain [4] reflectometry configurations. On the other hand, Brillouin scattering is potentially favorable compared to Rayleigh-based measurements, as it achieves simultaneously high spatial resolution and long measurement range. Up to now, two mechanisms were employed to determine the optical ERI from Brillouin measurements, relying either on the measurement of the Brillouin frequency shift (BFS) [5], or on the power reflected from a Brillouin dynamic grating (BDG) [6-8]. In the former case, as the BFS is retrieved with a typical accuracy of 1 MHz, the ERI estimate resolution is limited to ≈ $10^{-4}$. In Ref. [5], this resolution was sufficient to determine the ERI difference of adjacent modes, in virtue of the large $\Delta n_{eff}$ in that fiber. In commercial step-index or graded-index FMFs, the ERI difference between distinct modes may be too small to be resolved by BFS measurements only. In configurations based on BDG, a much finer birefringence resolution can be achieved (in the order of $10^{-7}$, typically [7, 8]). However, the setup is much more complex as it requires the use of separate laser sources and a coherent detection system.

In this paper, we show that ERI differences in the order of $10^{-7}$ can be recovered from Brillouin scattering measurements, using the same apparatus commonly used to retrieve the BFS distribution. Specifically, we show that the intermodal ERI difference can be determined through the Brillouin gain oscillations induced by multimodal interference (MMI). In our experiments, a commercial two-mode graded-index FMF was employed as the fiber under test. The modal birefringence between the $LP_{01}$ and $LP_{11}$ modal groups (MG), as well as the birefringence between the vector modes $TE_{01}$, $TM_{01}$ and $HE_{21}$, were determined with a 2-m spatial resolution. The experimental results have been validated by analyzing the fiber's Rayleigh-backscattered trace acquired with the Optical Frequency-Domain Reflectometer (OFDR) [4, 9].

## II. Theory

Stimulated Brillouin scattering (SBS) is a third-order optical nonlinear effect that can be easily observed in an optical fiber through a pump-probe technique [10]. In brief, launching a pump wave and a frequency-detuned probe wave at the two opposite ends of a fiber, a power coupling between the two waves occurs when their frequency shift satisfies the phase-matching condition:

$$BFS = \left(n_{eff,p} + n_{eff,s}\right)V_a/\lambda \quad (1)$$

where $n_{eff,p}$ and $n_{eff,s}$ are the ERIs of the pump and probe wave, respectively, $V_a$ is the acoustic velocity in the medium, and $\lambda$ is the wavelength of the pump in the vacuum. In a single-mode fiber the pump and probe waves propagate in the same spatial mode, therefore the ERIs of the pump and probe wave appearing in Eq. (1) are almost identical. Instead, in an FMF the two interacting beams can propagate either in the same spatial mode (intramodal Brillouin scattering), or in distinct spatial

E. Catalano, R. Vallifuoco. L. Zeni and A. Minardo are with the Department of Engineering, Università della Campania Luigi Vanvitelli. Via Roma 29, 81031 Aversa (Italy) (e-mail: aldo.minardo@unicampania.it).

M. Cappelletti, A. Galtarossa and L. Palmieri are with the Department of Information Engineering, University of Padova, 35131 Padova, Italy.

modes (intermodal Brillouin scattering) [11]. Equation (1) shows that, if the two beams are guided in the same spatial mode (i.e., in case of intramodal Brillouin scattering), their ERI can be estimated as:

$$n_{eff,i} = \frac{BFS,i}{2V_a}\lambda \quad (2)$$

where the index $i$ refers to the considered optical mode of the FMF. From Eq. (2), it is clear that two independent measurements of the BFS obtained by launching the pump and probe beams in one spatial mode, and then in another spatial mode, provide an estimate of the ERI difference between these two modes:

$$\Delta n_{eff(i,j)} = \frac{(BFS,i-BFS,j)}{2V_a}\lambda \quad (3)$$

In Eq. (3), $BFS,i$ and $BFS,j$ are the BFS measured by launching the pump and probe beams along the i-th and j-th mode, respectively. It is important to observe that, the use of Eq. (3) implies that the intramodal Brillouin scattering involving either the i-th or the j-th mode is mediated by the same acoustic wave, traveling with an acoustic velocity $V_a$. As FMF fibers also support multiple acoustic modes, the resulting Brillouin gain spectrum (BGS) is generally multipeaked [11], therefore special care must be taken in selecting the correct BFS. As a general rule, the intramodal Brillouin scattering between higher-order optical modes gives rise to a smaller BFS owing to their lower ERI, provided that the same acoustic mode is involved. Clearly, the limited resolution in the measurement of the BFS imposes a limit on the accuracy with which the ERI difference can be determined through Eq. (3). For example, assuming an acoustic velocity $V_a$ = 5800 m/s and a minimum detectable change of the BFS equal to 0.5 MHz, the use of Eq. (3) results in a minimum detectable modal birefringence $\Delta n_{eff,min}(BFS) \approx 1.3\cdot10^{-4}$. Clearly, the exact value will also depend on the adopted spatial resolution, where a finer resolution usually implies a higher uncertainty in the BFS estimate.

For smaller ERI differences, as the ones occurring between the vector modes of the same LP group in a standard FMF, the resolution in the BFS measurement may be not sufficient. Conveniently, another mechanism comes into play in Brillouin measurements involving more spatial modes: Let us assume that the pump beam is guided into the $LP_{01}$ ($HE_{11}$) mode, while the probe beam is distributed among the vector components of the $LP_{11}$ group (the $TE_{01}$, $TM_{01}$ and $HE_{21}$ modes). Due to the multimodal interference (MMI) between these three modes, the probe beam intensity will oscillate along the fiber with a spatial period (i.e., a beat length) depending on the ERI difference between the beating modes. Specifically, the probe beam intensity distribution along the fiber will contain different spatial frequencies, with each spatial frequency $f_{i,j}$ being given by:

$$f_{i,j} = \frac{n_{eff,i}-n_{eff,j}}{\lambda} \quad (4)$$

When the pump beam interacts with the probe beam due to intermodal SBS, the local Brillouin gain will depend on the intensity of the pump and probe beam in that position. Therefore, the measured Brillouin peak gain distribution will contain the same spatial frequencies of the probe intensity. This concept is similar to the one used in Ref. [12], where the Brillouin optical time-domain analysis was exploited to probe the power distribution of the four-wave mixing generated by two lasers. Based on Eq. (4), the ERI differences can be determined using:

$$\Delta n_{eff(i,j)} = f_{i,j}\cdot\lambda \quad (5)$$

where $f_{i,j}$ are the frequencies contained in the Brillouin gain spatial profile. Using a generic equipment for distributed Brillouin measurements, the Brillouin gain profile will be acquired with a certain spatial resolution and sampling rate, which influence the range of spatial frequencies that can be correctly retrieved from the measurements. Therefore, it is important to determine the spatial resolution required to recover the modal birefringence expressed by Eq. (5). According to the Nyquist criterion, the sampling frequency should be at least twice the spatial frequency. For a given spatial resolution SR, the maximum detectable modal birefringence will therefore be $\Delta n_{eff,max} = \lambda/2SR$. For example, for SR = 5 mm we get $\Delta n_{eff,max} \approx 1.5\cdot10^{-4}$. On the other hand, the minimum detectable modal birefringence will depend on the minimum detectable spatial frequency of the Brillouin gain profile, which in turns depends on the length of the fiber segment used to determine the Brillouin gain spatial frequencies. Assuming, e.g., an observation window (OW) of 2 m, Eq. (5) provides a minimum detectable modal birefringence $\Delta n_{eff,min} = f_{i,j,min}\cdot\lambda = \frac{\lambda}{OW} \approx 7.76\cdot10^{-7}$. Clearly, there is a trade-off between the length of the observation window (i.e., the granularity in modal birefringence measurements) and $\Delta n_{eff,min}$.

In summary, the two described mechanisms relating the Brillouin scattering measurements in FMFs with their modal birefringence show a complementary behavior: a higher ERI difference is beneficial when it comes to using Eq. (3), as it results in a wider separation between the corresponding BFSs, while it is detrimental when it comes to observing the MMI between the various modes, due to the limited spatial resolution of Brillouin measurements. Instead, the MMI is best observed when the optical modes have a smaller ERI difference. From a quantitative point of view, the Brillouin gain modulation induced by MMI along a FMF permits us to estimate, through intermodal SBS measurements, the modal birefringence in the range $\approx 10^{-7}$-$10^{-4}$, while higher birefringence values can be determined from the corresponding BFS shifts measured through intramodal SBS measurements.

## III. Experimental results

Distributed birefringence measurements have been carried out using the Brillouin Optical Frequency-Domain analysis (BOFDA) apparatus [13] shown in Fig. 1(a). The scheme utilizes an external-cavity diode laser (ECDL) emitting at 1550nm, with an output power of 16 dBm and a linewidth of 100 kHz, whose continuous-wave output is split by a 50/50 polarization-maintaining fused fiber optical coupler: one branch is modulated through the electro-optic Mach-Zehnder

modulator EOM1 driven by the output port of a vector network analyzer (VNA), and then amplified up to 19.6 dBm by an erbium-doped fiber amplifier (EDFA). The modulator EOM1 has a bandwidth of 20 GHz and is biased at the quadrature point. The output of the amplifier is sent to a polarization switch, and finally injected into the FMF as the pump beam. The polarization switch is employed to rotate alternatively the state-of-polarization (SOP) by $\pi/2$, so as to record the pump-probe interaction for two orthogonal states of the pump. Summing the two recordings, a compensation of the SOP dependence of the Brillouin gain is realized. The other branch is frequency-shifted through suppressed-carrier, double sideband modulation realized by another electro-optic modulator (EOM2), having the same bandwidth of EOM1 and driven by a RF synthesizer with an output power of 12 dBm. The two sidebands generated by EOM2 are amplified up to 16 dBm, and finally launched to the opposite end of the FMF. Two photonic lanterns (PL) (Phoenix Photonics), with three output ports corresponding to the $LP_{01}$, $LP_{11a}$, and $LP_{11b}$ modes and a nominal mode extinction > 15 dB, were used to selectively launch a single spatial mode group from the two ends of the FMF. By scanning the microwave frequency applied to the electro-optic modulator EOM2, the Brillouin gain spectrum (BGS) can be recorded for any pump-probe modal pair. The spatial resolution is dictated by the modulation frequency range swept by the VNA and can be as fine as 8 mm in our setup. The optical power of the probe light reaching the photodetector (Newport 1544-B) was close to its saturation power (≈ -3 dBm).

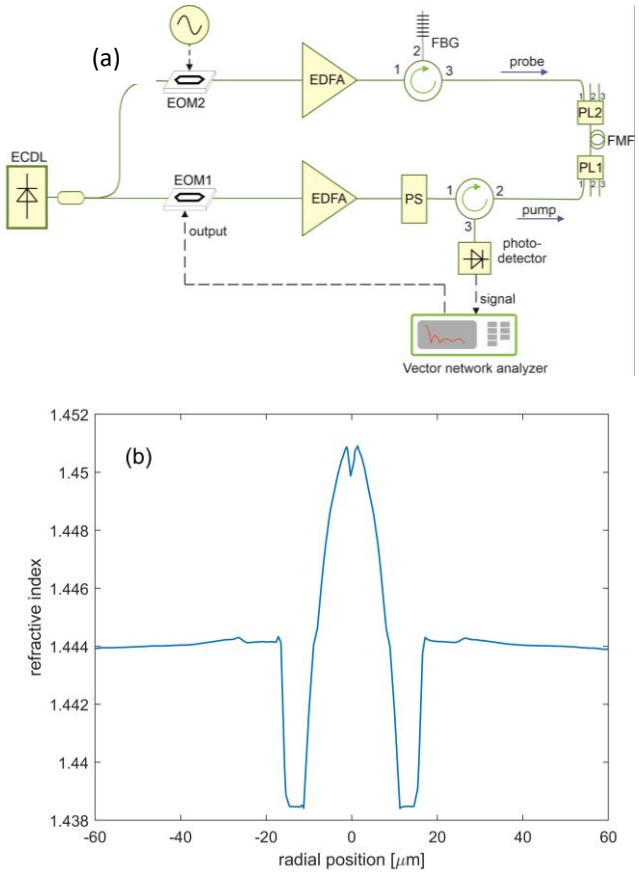


Fig. 1(a). BOFDA setup for distributed modal birefringence measurements in few-mode fibers; (b) Refractive index distribution of the investigated FMF.

The FMF chosen for our experiments is a ≈ 24-m long two-mode graded-index fiber (OFS, #80730). The refractive index profile along the radial position, as measured by an IFA-100 interferometric fiber analyzer, is plotted in Fig. 1(b). In Fig. 2(a), we report the BGS in a generic section of the FMF, as measured by launching the pump and probe beams either into the $LP_{01}$ (blue line) or $LP_{11a}$ (red line) ports of the two photonic lanterns, respectively (intramodal SBS). For completeness, the same figure also shows the BGS resulting from intermodal Brillouin scattering and measured by launching the pump into the $LP_{01}$ mode and the probe into the $LP_{11a}$ mode. All the spectra were acquired by sweeping the VNA modulation frequency up to 50 MHz, resulting in a spatial resolution of 2 m. Apparently, each BGS exhibits several peaks, because of the different acoustic modes supported by the FMF. Remarkably, the left-most peak of the BGS resulting from the $LP_{01}$-$LP_{01}$ scattering, denoted in Fig. 2(a) with $BFS_{01}$, differs by ≈ 20 MHz from the left-most peak of the BGS resulting from the $LP_{11a}$-$LP_{11a}$ scattering, denoted with $BFS_{11}$. Under the hypothesis that these two peaks originate from the same acoustic mode, Eq. (3) predicts a modal birefringence of ≈ $2.7 \cdot 10^{-3}$ (an acoustic velocity of 5775 m $s^{-1}$ was used for this calculation, as derived from the BFS of the fundamental resonance of the $LP_{01}$-$LP_{01}$ BGS). We also see that the highest peak in the BGS recorded with the pump and probe beams launched through the $LP_{11a}$ ports of the two PLs is not the leftmost one, i.e., it does not originate from the fundamental acoustic mode. That means that, in this case, a higher acousto-optic efficiency is obtained through a higher-order acoustic mode [11]. By evaluating the difference ($BFS_{01}$ – $BFS_{11}$) as a function of the fiber position, we obtain the modal birefringence distribution shown in Fig. 2(b). In detail, the figure shows the modal birefringence distribution obtained by averaging the four distributions measured by launching the pump and probe beams through either the $LP_{11a}$ or $LP_{11b}$ ports. The same figure also reports the standard deviation over the four acquisitions, as calculated for each fiber position. Note that, the standard deviation of ($BFS_{01}$ – $BFS_{11}$), averaged along the whole fiber, is ≈ 5.3 MHz, corresponding to an uncertainty of ≈ $7.2 \cdot 10^{-4}$ in terms of modal birefringence. Most of this uncertainty comes from the measurement of the $BFS_{11}$, whose related peak is ≈ 14 dB weaker than the peak related to $BFS_{01}$ measurements (see Fig. 2(a)). The time required to perform each BFS profile acquisition was less than 1 minute, as determined by the number of sensing points, the IF bandwidth (10 kHz), and the range of pump-probe frequency shifts swept for each acquisition (from 10650 MHz to 11000 MHz at 2-MHz step).

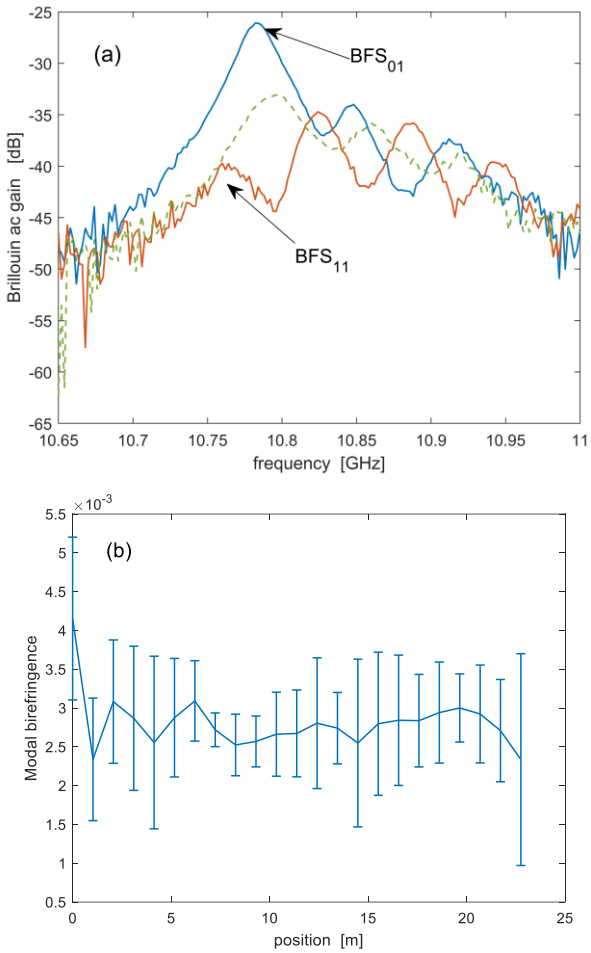


Fig. 2. (a) Intramodal and intermodal Brillouin gain spectra of the FMF (pump and probe on the $LP_{01}$ mode: blue line; pump and probe on the $LP_{11a}$ mode: red line; pump on the $LP_{01}$ mode and probe on the $LP_{11a}$ mode: green dashed line); (b) modal birefringence calculated using Eq. (3), with the error bars indicating the standard deviation over four acquisitions at each fiber position.

The setup shown in Fig. 1 was also used to capture the Brillouin gain variations along the FMF, observed by launching the pump beam into the $LP_{01}$ guided mode, and the probe beam into the $LP_{11a}$ mode (intermodal Brillouin scattering). In this case, the spatial resolution of the BOFDA measurement was set to 8 mm, i.e., the VNA modulation frequency was swept up to 12.8 GHz. The measurement time, in this case, was about 5 minutes, because of the higher number of spatially resolved points along the FMF. Note that, apart from the different connection of the PL ports, the measurement of the Brillouin gain involves the same steps required by conventional BFS measurements: the pump/probe frequency shift is swept over a proper range to acquire the BGS at each position; finally, each BGS is fitted by a Lorentz curve to extract the local Brillouin gain peak. As explained in the previous section, the modal birefringence related to the three vector components of the $LP_{11a}$ mode group gives rise to spatial variations of the Brillouin gain peak, as shown in Fig. 3(a). The same figure shows, in the inset, the spectrum obtained by applying a fast-Fourier transform (FFT) to the 2-m observation window highlighted in red (note that, the choice of a 2-m observation window resulted in a number of 250 sampling points inside each window, owing to the 8-mm spatial resolution). Three peaks are observed in the computed spectrum (apart from the additional peak due to the dc component), located at 2.93, 9.76 and 12.69 $m^{-1}$, respectively. Apparently, the frequency of the third peak equals the sum of the first two. According to our theory, these peaks result from the MMI among the three vector components of the $LP_{11a}$ mode group. The ERI differences, computed using Eq. (5), are $4.54 \cdot 10^{-6}$, $1.51 \cdot 10^{-5}$, and $1.97 \cdot 10^{-5}$ respectively. Note that these birefringence values are far too small to produce an appreciable BFS shift, therefore they could not be measured even if launching selectively the vector modes as in Ref. [5].

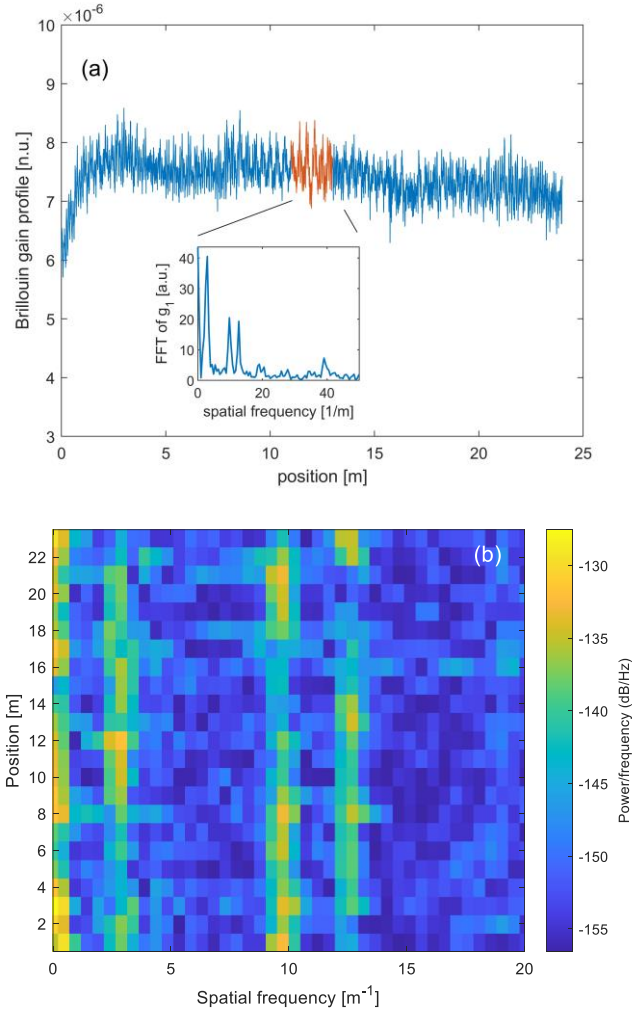


Fig. 3. (a) Spatial distribution of the Brillouin gain acquired by intermodal Brillouin scattering (pump: $LP_{01}$ mode; probe: $LP_{11a}$ mode). The inset shows the FFT of the portion of the Brillouin gain distribution highlighted in red; (b) Spectrogram of the Brillouin gain distribution.

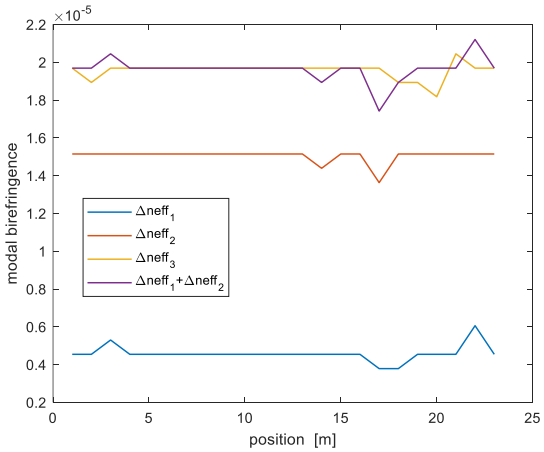


Fig. 4. Modal birefringence calculated from the spectral position of the peaks shown in Fig. 3(b), using Eq. (5).

Figure 3(b) shows the spectrogram of the Brillouin gain profile shown in Fig. 3(a), as calculated using a sliding window of 2 m and a 50% overlap between segments. We see that, still excluding the first leftmost peak attributed to the dc component, the remaining three peaks are observed all along the fiber at the same spatial frequencies. We report in Fig. 4 the spatial distribution of the modal birefringence computed from the spectral position of these peaks using Eq. (5). The same plot also shows the birefringence distribution computed by summing the first two peaks. Clearly, the position of the third peak corresponds to the sum of the first two ones, except for the discrepancy due to the uncertainty in the estimate of the peaks' position. We note that the spatial frequency resolution in the determination of the peaks is 0.5 $m^{-1}$ (owing to the 2-m observation window used for spectrogram calculation), which corresponds to a modal birefringence resolution of $7.76 \cdot 10^{-7}$ (see Eq. (5)). Clearly, a better resolution could be obtained by adopting a larger observation window, at the expense of a coarser granularity in the modal birefringence measurement. Note that, the same kind of measurement was carried out by launching the probe light into the $LP_{11b}$ mode, giving rise to results very similar to the ones shown in Fig. 3-4. In fact, the mode groups $LP_{11a}$ and $LP_{11b}$ are almost degenerate, and their modal birefringence is too small to be measured with our ERI resolution.

In order to support the modal birefringence estimates obtained by the proposed method, the same piece of fiber was characterized using the methods demonstrated in Refs. [4, 9]. The experimental setup, in this case, consists of a polarization sensitive OFDR equipped with a switching network and a PL, which enables the selection of the launched MG without perturbing the fiber. This approach ensures that each MG's unique Rayleigh signature generated by the FMF can be obtained through sequential measurements, while the fiber remains stable throughout the process. In this setup, a typical measurement can be represented by the $LP_i \rightarrow LP_j$ notation, where the first element indicates the port of the PL from which the probing light is injected into the fiber, while the second element refers to the port from which the Rayleigh scattering is measured. Ref. [4] explains how Rayleigh scattering produces mode-signatures in the fiber. By cross-correlating two distinct modes, a spectral shift is retrieved, which enables the calculation of the modal birefringence. To determine the relative modal birefringence between different mode pairs, a spectral correlation analysis (SCA) [4] is conducted by spectrally cross-correlating two Rayleigh measurements. For example, to compute the modal birefringence between $LP_{11}$ and $LP_{01}$, the best choice is to cross-correlate the measurement $LP_{01} \rightarrow LP_{01}$ with $LP_{11a} \rightarrow LP_{11a}$. As detailed in Ref. [4], to perform the SCA, two observation windows of length $w$ are slidden along the backscattered traces, with a possible relative delay. For each position $t$ of the windows (where $t = z/(2v_g)$ denotes the roundtrip delay from position $z$, considering an average group velocity $v_g$) the spectra of the trace are computed and cross-correlated. Whenever a peak occurs at a specific frequency, it means that the modal birefringence between the two modes $LP_{01}$, $LP_{11a}$ is $\Delta n = n_0 \Delta f / f_0$, $f_0$ being the central optical frequency of the OFDR scan (about 1550 nm). Note that all the extracted quantities depend on the choice of a reference refractive index $n_0$, here assumed equal to 1.466.

The results obtained from the SCA procedure to the fiber under test are shown in Fig. 5, where we have applied a sliding window of 2 cm. Note that, the fiber length in Fig. 5 was only 12 m, against the 24 m of previous tests. This discrepancy is due to the fact that about half the original FMF length was consumed due to consecutive tests and splices.

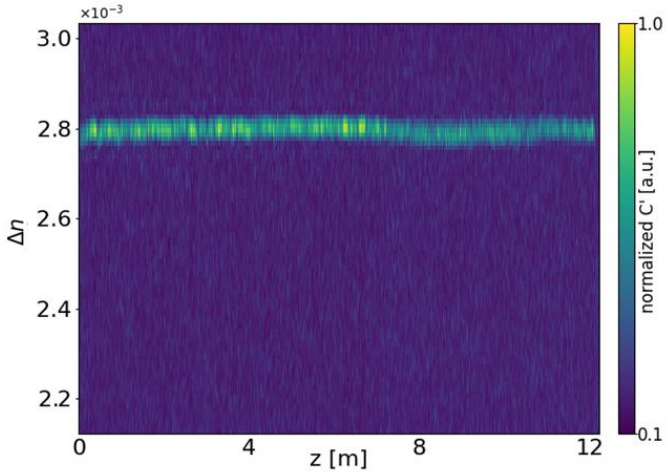


Fig. 5. Modal birefringence between mode groups $LP_{01} - LP_{11a}$.

In Fig. 5 we see an almost constant peak at $\Delta n \approx 2.79 \times 10^{-3}$, which is in good agreement with the ERI measured with the BOFDA approach. Analogously to what discussed above for the Brillouin gain oscillation measurements, the SCA applied between the $LP_{01}$ and the $LP_{11b}$ gave a very similar graph.

Rayleigh backscattered light can be also analyzed by a second approach, based on the evaluation of the coherency matrix of the total backscattered field [9]. According to this method, the Rayleigh backscatter excited by the light launched through one of the ports of the PL, is collected through the different ports of the same PL. Furthermore, for each collecting port the backscattering traces related to two orthogonal states-of-polarization are separately acquired. Thus, for our three-port PL we record a total of six complex amplitudes (3 spatial modes and 2 polarization modes for each spatial mode), that we

represent with the column vector $b(z)$. The coherency matrix is then defined as $B(z) = \langle b(z)b^*(z)\rangle_w$ ,where * denotes transposition and conjugation, and $\langle\cdot\rangle_w$ denotes the spatial average over the observation window of length $w$ [15]. In practice, the element of position $(i,j)$ of $B(z)$ is the spatial average of the beating between the light backscattered into port $i$ of the photonic lantern and the light backscattered into port $j$. As shown in Ref. [15], the elements of the coherency matrix have oscillations with spatial frequencies related to the modal birefringence. As an example, Fig. 6 displays the elements of the $6 \times 6$ coherency matrix measured by launching the light through the port 1 of our PL (each graph is normalized to its own maximum for clarity). Since the coherency matrix is Hermitian, the real part of the matrix elements is presented in blue in the upper triangle of the table in Fig. 6, while the imaginary parts are shown in red in the lower triangle. The rich spatial features are indicative of the coupling occurring among the modes and can be quantified by evaluating the power spectral density (PSD).

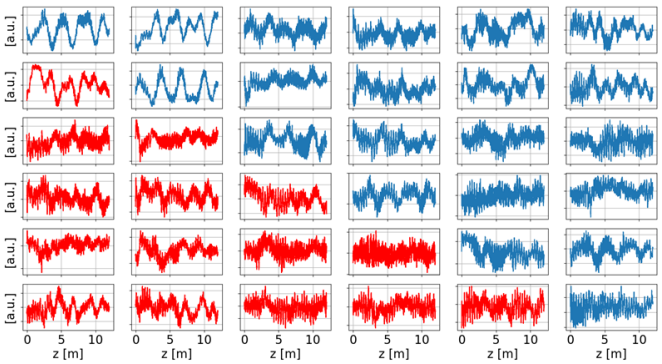


Figure 6. Coherency matrix $B(z)$ measured when the fiber is illuminated from input port 1 of the photonic lantern. The $i$th graph on the $j$th column is the element of position $(i,j)$ of $B(z)$. Since the coherency matrix is Hermitian, the real part of the matrix elements is presented in blue, while the imaginary parts are shown in red.

Figure 7 shows the PSD estimated on 2-m-long sections and averaged among all the coherency matrix elements. The peak at the lowest frequency corresponds to polarization beating within the $LP_{01}$ group, and relates to the slow oscillations visible in the top-left 2-by-2 block of Fig. 6. The other three strongest peaks are differently related to the beating between the three vector components of the $LP_{11}$ group. The corresponding modal birefringence $\Delta n$ (reported in the legend) are in very good agreement with the values obtained from the Brillouin analysis, confirming the reliability of the approaches. Finally, the other three smaller peaks are second-order harmonics associated to the previous ones and are a natural consequence of the round-trip propagation.

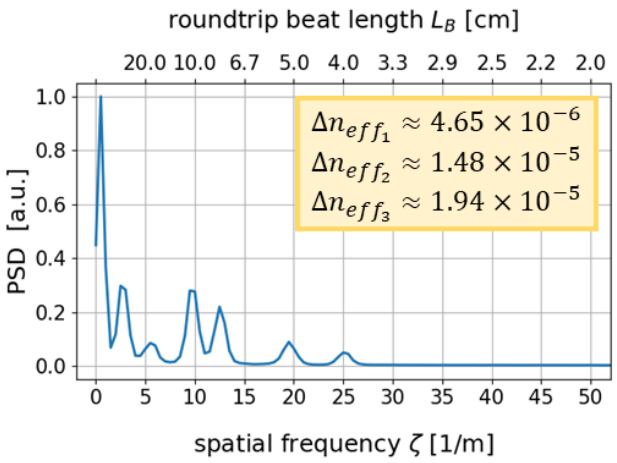


Figure 7. PSD estimated on 2-m-long sections and averaged among all the coherency matrix elements.

## IV. Conclusions

A novel method for distributed modal birefringence measurements in few-mode optical fibers has been proposed and experimentally validated. The method employes the Brillouin Optical Frequency-Domain Analysis and two photonic lanterns, by which the pump and probe lights involved in the Brillouin scattering process can be selectively launched into one of the mode groups supported by the FMF. The method has been validated using another apparatus making use of a totally different approach (Rayleigh scattering). The measurements obtained using the newly proposed method are in good agreement with the ones obtained using OFDR. Compared to the latter, the Brillouin-based method is potentially favorable as it can be applied to longer fibers. In particular, the maximum fiber length that can be investigated using our approach is limited to a few km's, due to the frequency-dependent pump depletion [16]. For fiber lengths of 10's of kms or more, BOFDA sensing is still possible, but the pump and probe powers must be much lower (<< 1mW [17]) than those used in our tests. In turn, this would limit the spatial resolution to a few meters, preventing the measurement of the MMI-induced spatial fluctuations of the Brillouin gain for the typical FMF modal birefringence.

Brillouin and Rayleigh scattering in optical fibers are known to be dependent on strain and temperature, a feature successfully exploited for distributed sensing in single-mode fibers [18]. With respect to single-mode fibers, few-mode fibers may potentially allow the separation of the contributions from temperature and strain, enabling multi-parameter sensing. In this perspective, a few preliminary studies have reported interesting, yet not conclusive, results [19-21]. Sensing is outside the scope of this paper. For this reason and to avoid measurement artifacts, the measurements presented here have been performed in conditions of constant temperature and strain. Nevertheless, the proposed method may potentially be applied not only for fiber characterization, but also for sensing.

## References

[1] R. Ryf *et al.*, "Mode-division multiplexing over 96 km of few-mode fiber using coherent 6 × 6 mimo processing," *J. Lightw. Technol.*, vol. 30, no. 4, pp. 521–531, Feb 2012.

[2] Y. Xu, M. Ren, Y. Lu, P. Lu, P. Lu, X. Bao, L. Wang, Y. Messaddeq, and S. LaRochelle, "Multi-parameter sensor based on stimulated Brillouin scattering in inverse-parabolic graded-index fiber," *Opt. Lett.*, vol. 41, no. 6, pp. 1138-1141, 2016.

[3] K. Markiewicz, L. Szostkiewicz, J. Kaczorowski, Z. Yang, A. Dominguez-Lopez, M. Napierała, T. Nasiłowski and L. Thévenaz, "Distributed measurement of mode group effective refractive index difference in a few mode optical fibers," *Opt. Express*, vol. 30, no. 10, pp. 17164-17173, 2022.

[4] R. Veronese, A. Galtarossa and L. Palmieri, "Distributed Characterization of Few-Mode Fibers Based on Optical Frequency Domain Reflectometry," *J. of Lightw. Technol.*, vol. 38, no. 17, pp. 4843-4849, Sept. 2020.

[5] P. Pradhan, D. Sengupta, L. Wang, C. Tremblay, S. LaRochelle and B. Ung, "The Brillouin gain of vector modes in a few-mode fiber," *Sci. Rep.*, vol. 7, 1552, 2017.

[6] S. Li, M.-J. Li and R. S. Vodhanel, "All-optical Brillouin dynamic grating generation in few-mode optical fiber," *Opt. Lett.* Vol. 37, pp. 4660-4662, 2012.

[7] A. Li, Q. Hu, X. Chen, B. Y. Kim and W. Shieh, "Characterization of distributed modal birefringence in a few-mode fiber based on Brillouin dynamic grating," *Opt. Lett.*, vol. 39, no. 11, pp. 3153-3156, 2014.

[8] Y. H. Kim and K. Y. Song, "Distributed Analysis on the Spatial Mode Structure in a PANDA-Type Few-Mode Fiber By Brillouin Dynamic Gratings," *J. of Lightw. Technol.*, vol. 39, no. 2, pp. 612-619, Jan. 2021.

[9] M. Cappelletti *et al.* "Distributed Polarization and Coupling Analysis of a 3-Coupled-Core Fiber", Optical Fiber Communication Conference (OFC), paper W1C.3 (2023).

[10] A. Kobyakov, M. Sauer and D. Chowdhury, "Stimulated Brillouin scattering in optical fibers," *Adv. Opt. Photon.*, vol. 2, pp, 1–59, 2010.

[11] K. Y. Song and Y.H. Kim, "Characterization of stimulated Brillouin scattering in a few-mode fiber," *Opt. Lett.*, vol. 38, no. 22, pp. 4841-4844, 2013.

[12] M. González Herráez, L. Thévenaz and P. Robert, "Distributed measurement of chromatic dispersion by four-wave mixing and Brillouin optical-time-domain analysis," *Opt. Lett.*, vol. 28, no, 22, pp. 2210-2212, 2003.

[13] R. Bernini, A. Minardo and L. Zeni, "Distributed Sensing at Centimeter-Scale Spatial Resolution by BOFDA: Measurements and Signal Processing," *IEEE Photon. J.*, vol. 4, no. 1, pp. 48-56, 2012.

[14] A. Kobyakov *et al.*, "Design concept for optical fibers with enhanced SBS threshold," *Opt. Express*, vol. 13, no. 14, pp. 5338-5346, 2005.

[15] C. Antonelli, A. Mecozzi, M. Shtaif and P. J. Winzer, "Stokes-space analysis of modal dispersion in fibers with multiple mode transmission," *Opt. express*, vol. 20, no. 11, pp. 11718-11733, 2012.

[16] A. Minardo, R. Bernini and L. Zeni, "A Simple Technique for Reducing Pump Depletion in Long-Range Distributed Brillouin Fiber Sensors," *IEEE Sens. J.*, vol. 9, no. 6, pp. 633-634, June 2009.

[17] T. Kapa, A. Schreier; K. Krebber, "A 100-km BOFDA Assisted by First-Order Bi-Directional Raman Amplification," Sensors 2019, 19, 1527. https://doi.org/10.3390/s19071527

[18] A. Hartog, An Introduction to Distributed Optical Fibre Sensors. CRC Press, 2018.

[19] H. Wu *et al.* "Few-mode optical fiber based simultaneously distributed curvature and temperature sensing," *Opt Express*, vol. 29, no. 25, pp. 12722-12732, May 2017.

[20] A. Li, Y. Wang, J. Fang, M.-J. Li, B. Y. Kim and W. Shieh, "Few-mode fiber multi-parameter sensor with distributed temperature and strain discrimination," *Opt. Lett.*, vol. 40, pp. 1488-1491, 2015.

[21] R. Veronese, M. Santagiustina, A. Galtarossa, and L. Palmieri, "Experimental characterization of perturbation-induced modal birefringence in few-mode fibers", in ECOC 2019; European Conference on Optical Communication, Dublin, Ireland, 2019.